Nanotube templates

Synthesis of TaS_2 Nanotubes From Ta_2O_5 Nanotube Templates**

*Phoebe Li, Christopher L. Stender, Emilie Ringe, Laurence D. Marks, and Teri W. Odom**

The discovery that layered transition metal dichalcogenide (TMD) materials such as WS_2[1] and MoS_2[2] can form nanotubes and other inorganic fullerene-type structures has generated considerable interest in the study and synthesis of nanomaterials consisting of two-dimensional (2D), layered structures.[3–5] One unique property of TMD nanomaterials includes superior tribological behavior;[6] other applications include use as solid lubricants,[7] catalysts for hydrosulfurization,[8] and hydrogen-storage devices.[9] Control over the nanoscale architecture could also greatly accelerate investigations of finite size effects on complex electronic properties such as superconductivity and charge-density wave (CDW) behavior. For example, tantalum disulfide (TaS_2) displays three polytypes where Ta atoms are covalently bonded between two layers of S atoms in trigonal prismatic (2H), octahedral (1T), or mixed (6R) coordinations.[10] Investigations of structure–property relationships of TaS_2 nanomaterials have been limited, however, because they can neither be produced in high yield nor with control over the crystalline structure.

Tubular TaS_2 nanomaterials have been synthesized by the hydrogen reduction of TaS_3 precursors[11] but the crystal structure could not be determined because of sample degradation under the electron beam. Other nanostructures of TaS_2 include fullerene-like TaS_2 nanoparticles produced by a gas-phase reaction[12] and TaS_2 nanoplates formed by laser ablation[13] or from molecular precursors.[14] 2H-TaS_2 nanowires synthesized from elemental Ta and S by chemical vapor transport exhibited a superconductivity transition temperature ($T_c = 3.4$ K) higher than that of bulk 2H-TaS_2 (0.8 K).[15] Recently, we demonstrated synthetic control over the size, shape, and polytype of surface-patterned TaS_2 nanostructures by converting nanopatterned tantalum oxide (Ta_2O_5) to TaS_2 using a gas-phase reaction.[14]

Here we report how large quantities of crystalline TaS_2 multi-walled nanotubes can be synthesized starting from Ta_2O_5 nanotube templates. We achieved control over the length, diameter, and the number of TaS_2 layers within the nanotube. Our template-based approach produced a high yield of structurally uniform nanotubes, which opens up possibilities for potential scalable applications. Also, we observed that the electronic properties were different from the bulk, where the T_c of the TaS_2 nanotubes was elevated, and the CDW transition temperature (T_{CDW}) was suppressed.

Figure 1a depicts the scheme for converting Ta_2O_5 nanotubes to multi-walled TaS_2 nanotubes. First, large-area arrays ($\approx 3.5 \times 10^{10}$ tubes cm^{-2}) of amorphous Ta_2O_5

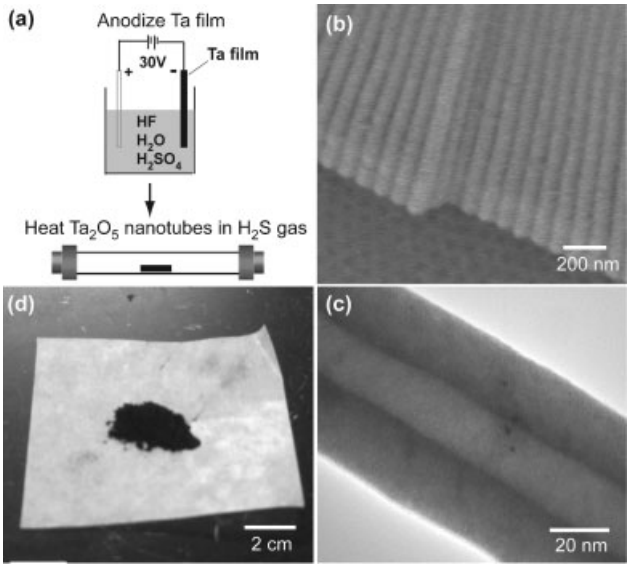

Figure 1. a) Scheme of chemical conversion process to synthesize TaS_2 nanotubes starting from Ta_2O_5 nanotube templates. b) SEM image of Ta_2O_5 nanotube arrays formed after anodizing the Ta film. c) TEM image of a Ta_2O_5 nanotube. d) Photograph of bulk quantities of TaS_2 nanotubes.

[*] Prof. L. D. Marks, Prof. T. W. Odom
Department of Materials Science and Engineering
Northwestern University
2145 Sheridan Road, Evanston, IL 60208 (USA)
E-mail: todom@northwestern.edu
P. Li
Department of Chemical Engineering
Northwestern University
2145 Sheridan Road, Evanston, IL 60208 (USA)
Dr. C. L. Stender, E. Ringe, Prof. T. W. Odom
Department of Chemistry
2145 Sheridan Road, Evanston, IL 60208 (USA)

[**] This work was supported by the NSF CAREER Award (CHE-0349302) and the David and Lucile Packard Foundation. This work used the NUANCE Center facilities, which are supported by NSF-MRSEC, NSF-NSEC, and the Keck Foundation as well as the J. B. Cohen X-Ray Diffraction Facility supported by the MRSEC program of the National Science Foundation (DMR-0520513) at the Materials Research Center of Northwestern University. The authors also thank Dr. O. Chernyashevskyy at the Magnetic and Physical Properties Measurement Facility for useful discussions.

DOI: 10.1002/smll.201000226

nanotubes (Figure 1b) were grown by the electrochemical anodization of a 300-μm-thick Ta film (Aldrich, 99.9%) in a room-temperature solution of HF:H_2SO_4 (2 mL 48% HF, 50 mL 85% H_2SO_4) at 30 V for 10 min.[16] Ta_2O_5 nanotubes were washed repeatedly with deionized water to remove all traces of H_2SO_4 and then vacuum filtered. Transmission electron microscopy (TEM, JEOL JEM-2100F, 200 kV) revealed that Ta_2O_5 nanotubes synthesized under these conditions were 10–13 μm long, 60–70 nm in diameter, and 15–20 nm in wall thickness (Figure 1c). The dried samples were placed in a 13″ quartz tube furnace for sulfidization and heated at a rate of 2 °C min^{-1} to 625 °C under 16 sccm of 99.5% H_2S(g).The reaction time controls the number of TaS_2 layers formed within the nanotube. A 24 h reaction time was enough to convert the Ta_2O_5 nanotubes completely into multi-walled TaS_2 nanotubes. The furnace was then cooled to ambient temperature, and a black powder was obtained (Figure 1d).

Glancing-angle X-ray diffraction (GA-XRD) patterns (Rigaku ATX-G, 18 kW Cu source) of the sample were consistent with 2H-TaS_2 (PDF 01-080-0685), with lattice parameters $a = 3.314$ Å, $b = 3.314$ Å, $c = 12.097$ Å (Figure 2a). TEM images show that fully converted tubes had approximately 25 layers of TaS_2 stacked along the *c*-axis (Figure 2b).The electron-diffraction patterns show prominent rings that correspond to randomly oriented (101) and (106) planes of TaS_2 along the length of the nanotube (Figure 2c). The intense (002) spots aligned perpendicular to the nanotube axis corresponded to the *c*-axis spacing between the layers, which was calculated to be 6.07 ± 0.03 Å. This result is in good agreement with the interlayer spacing of 2H-TaS_2 (6.05Å)[12] and further supports that the TaS_2 nanotube polytype was 2H.

Unlike other synthetic approaches, our method allows nanotubes to be formed with varying numbers of TaS_2 layers depending simply on the reaction time. We synthesized TaS_2 nanotubes at three different conversion times (1 h, 4 h, and 12 h) to gain insight into the reaction mechanism. GA-XRD patterns of the intermediate times showed that as the conversion time increased from 1 h to 12 h, the initially amorphous Ta_2O_5 nanotube template exhibited highly crystalline Ta_2O_5 peaks at 4 h, which were then gradually replaced by the characteristic (002), (100), and (106) TaS_2 peaks at 12 h and 24 h as the sulfidization reaction progressed (Figure 3). This increase in peak intensity corresponds to the growing number of TaS_2 layers along the *c*-axis as the conversion time increased.

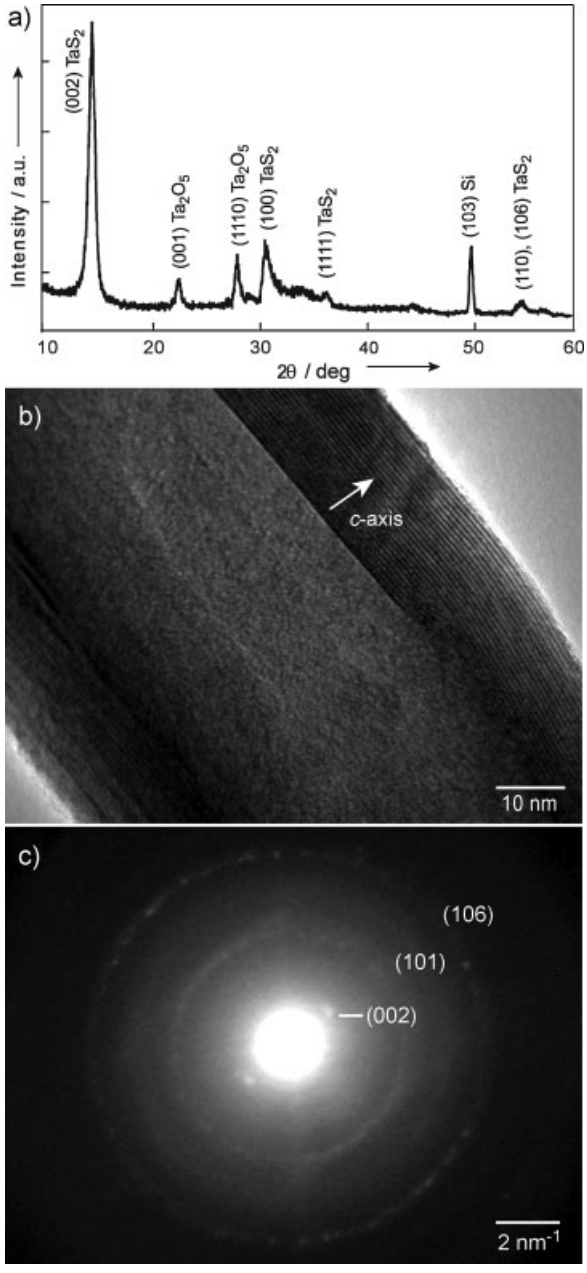

Figure 2. Structural characterization of TaS_2 nanotubes after 24 h reaction. a) GA-XRD spectra. b) TEM image of a single nanotube. c) Electron diffraction pattern of a single nanotube using a 1.4-μm-radius illumination disc.

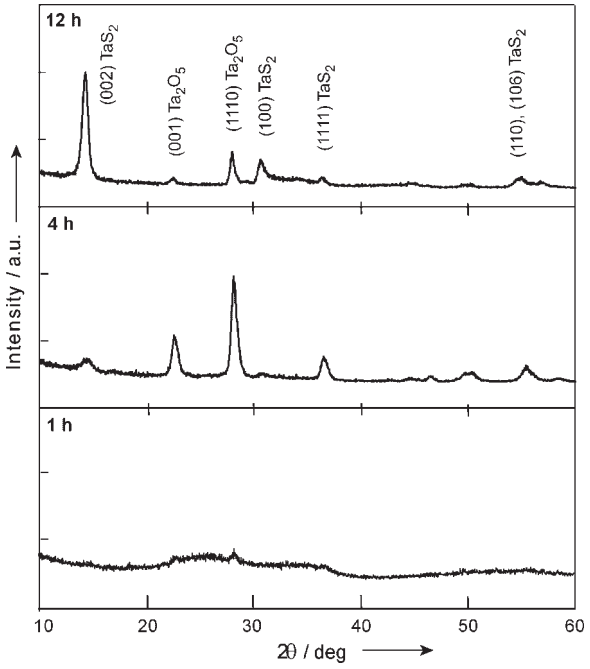

Figure 3. GA-XRD spectra of TaS_2 nanotubes at different conversion times in H_2S(g). After 12 h, there is still some residual yet crystalline Ta_2O_5, which is most likely in the center of the nanotube.

TEM images confirmed that the average number of metal disulfide layers depended on the reaction time. After 1 h, <5 TaS_2 layers formed on the interior and exterior surfaces of the amorphous Ta_2O_5 nanotube. The layers were discontinuous and did not connect along the entire length of the nanotube (Figure 4a). After 4 h of conversion, more TaS_2 layers were formed (10–15) and started to connect along the length of the nanotube (Figure 4b). Electron diffraction patterns were indexed to (002), (101), and (106) TaS_2, as well as (002) Ta_2O_5, which indicated the presence of unreacted oxide. At 12 h of conversion, TaS_2 layers continued to form along the *c*-axis (Figure 4c). The relative intensity of the (002) Ta_2O_5 feature in the 12 h electron diffraction pattern decreased because of the conversion of Ta_2O_5 to TaS_2. After 24 h, the entire Ta_2O_5 wall was converted to layers of TaS_2 (25 ± 5), resulting in the multilayered structure of the nanotubes (Figure 2b). The (002) Ta_2O_5 ring was undetectable in the 24 h electron diffraction pattern. The reaction time-dependent TEM images suggest a diffusion-controlled process that progresses from both the interior and exterior of the nanotube towards the center. This mechanism is consistent with the residual Ta_2O_5 present in the 24-h nanotubes in the GA-XRD spectrum (Figure 2a).

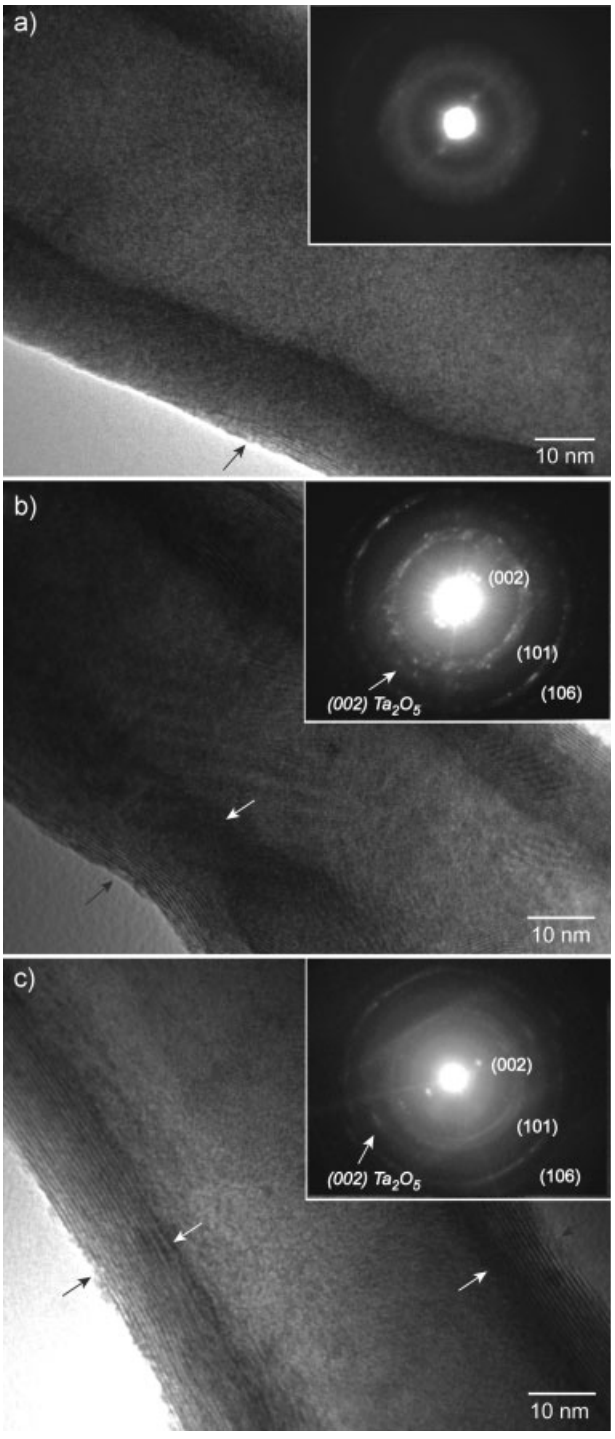

Figure 4. TEM images and electron diffraction patterns (insets) of TaS_2 nanotubes converted for a) 1 h, b) 4 h, c) 12 h. White arrows indicate inner TaS_2 walls and black arrows indicate outer TaS_2 walls.

Superconductivity and CDW behavior have been observed to be competing mechanisms in bulk layered dichalcogenides such as Cu_xTiSe_2[17] and $NbSe_2$.[18] $NbSe_2$ nanotubes have been shown to be superconducting at low temperatures,[19] and calculations have predicted that NbS_2 nanotubes will exhibit superconducting behavior different to that of the bulk.[20] Our template-based method offers an ideal approach to design a model system for studying the effects of nanoscale structure on electronic properties in reduced dimensions. Bulk 2H-TaS_2 is known to be superconducting below $T_c = 0.8$ K[10] and to exhibit an incommensurate CDW transition around $T_{CDW} = 75$ K.[10] TaS_2 nanowires and nanobelts have shown an elevated T_c;[15,21] however, there are no reports on measurements of both T_c and T_{CDW} for the same TaS_2 nanomaterial, and no investigations on how the electronic properties depend on the finite number of TaS_2 layers. We used a superconducting quantum interference device (SQUID) to characterize the electronic behavior of 4 h and 24 h nanotubes. Zero-field-cooled (ZFC) measurements at low field ($H = 10$ Oe) revealed a T_c of 2.3 K and 2.8 K, respectively (Figure 5), which is higher than bulk T_c. ZFC measurements at high field ($H = 500$ Oe) showed a strong peak at 63 K for 24 h tubes, which is less than bulk T_{CDW}, while the 4 h nanotubes did not exhibit any features (Figure 5, inset). One possible reason for the low signal of 4 h tubes could be the low quantities of TaS_2 in partially converted tubes.

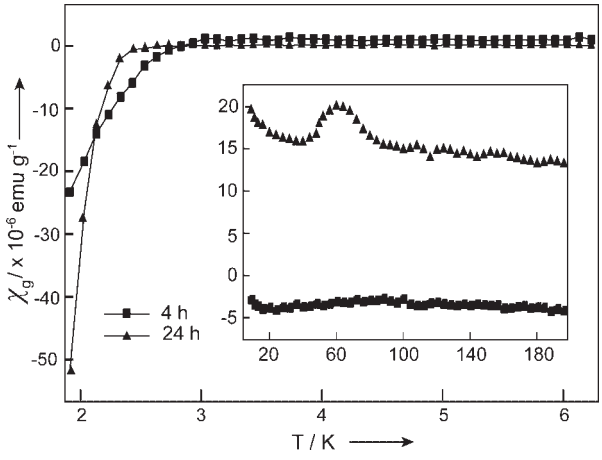

Figure 5. Superconductivity measurements of TaS_2 measurements at low field ($H = 10$ Oe). Inset: CDW measurements at high field ($H = 500$ Oe).

In summary, we have demonstrated a simple method to synthesize multi-walled 2H-TaS_2 nanotubes in high yield from Ta_2O_5 nanotube templates with control over the length, diameter, and the number of TaS_2 layers. These nanotubes exhibit superconductivity and CDW behavior different from bulk TaS_2. We anticipate that this template-based method can be readily applied to synthesize other TMD nanotubes from the appropriate precursors, and advance the study of TMD materials in reduced dimensions.

Keywords:
chalcogenides · nanotubes · superconductors · tantalum sulfide · templates

[1] R. Tenne, L. Margulis, M. Genut, G. Hodes, *Nature* **1992**, *360*, 444.
[2] Y. Feldman, E. Wasserman, D. J. Srolovitz, R. Tenne, *Science* **1995**, *267*, 222.
[3] R. Tenne, *Nat. Nanotechnol.* **2006**, *1*, 103.
[4] R. Tenne, G. Seifert, *Ann. Rev. Mater. Res.* **2009**, *39*, 387.
[5] C. N. R. Rao, A. Govindaraj, *Adv. Mater.* **2009**, *21*, 4208.
[6] I. Kaplan-Ashiri, S. R. Cohen, K. Gartsman, V. Ivanovskaya, T. Heine, G. Seifert, I. Wiesel, H. D. Wagner, R. Tenne, *Proc. Natl. Ac. Sci. USA* **2006**, *103*, 523.
[7] L. Rapoport, Y. Bilik, Y. Feldman, M. Homyonfer, S. R. Cohen, R. Tenne, *Nature* **1997**, *387*, 791.
[8] F. Y. Cheng, J. Chen, X. L. Gou, *Adv. Mater.* **2006**, *18*, 2561.
[9] J. Chen, N. Kuriyama, H. Yuan, H. T. Takeshita, T. Sakai, *J. Am. Chem. Soc.* **2001**, *123*, 11813.
[10] J. A. Wilson, F. J. Disalvo, S. Mahajan, *Phys. Rev. Lett.* **1974**, *32*, 882.
[11] M. Nath, C. N. R. Rao, *J. Am. Chem. Soc.* **2001**, *123*, 4841.
[12] C. Schuffenhauer, B. A. Parkinson, N. Y. Jin-Phillipp, L. Joly-Pottuz, J. M. Martin, R. Popovitz-Biro, R. Tenne, *Small* **2005**, *1*, 1100.
[13] K. Y. Chick, M. Nath, B. A. Parkinson, *J. Mater. Res.* **2006**, *21*, 1243.
[14] C. L. Stender, P. Sekar, T. W. Odom, *J. Solid State Chem.* **2008**, *181*, 1621.
[15] C. W. Dunnill, H. K. Edwards, P. D. Brown, D. H. Gregory, *Angew. Chem. Int. Ed.* **2006**, *45*, 7060.
[16] J. Barton, C. L. Stender, P. Li, *J. Mater. Chem.* **2009**, *19*, 4896.
[17] E. Morosan, H. W. Zandbergen, B. S. Dennis, J. W. G. Bos, Y. Onose, T. Klimczuk, A. P. Ramirez, N. P. Ong, R. J. Cava, *Nat. Phys.* **2006**, *2*, 544.
[18] D. J. Huntley, *Phys. Rev. Lett.* **1976**, *36*, 490.
[19] M. Nath, S. Kar, A. K. Raychaudhuri, C. N. R. Rao, *Chem. Phys. Lett.* **2003**, *368*, 690.
[20] G. Seifert, H. Terrones, M. Terrones, T. Frauenheim, *Solid State Comm.* **2000**, *115*, 635.
[21] X. C. Wu, Y. R. Tao, Y. M. Hu, Y. Song, Z. Hu, J. J. Zhu, L. Dong, *Nanotechnology* **2006**, *17*, 201.

Received: February 10, 2010

